www.sciencemag.org/content/352/6281/91/suppl/DC1

Supplementary Materials for

A long noncoding RNA associated with susceptibility to celiac disease

Ainara Castellanos-Rubio, Nora Fernandez-Jimenez, Radomir Kratchmarov, Xiaobing Luo, Govind Bhagat, Peter H. R. Green, Robert Schneider, Megerditch Kiledjian, Jose Ramon Bilbao, Sankar Ghosh*

*Corresponding author. E-mail: sg2715@columbia.edu

Published 1 April 2016, *Science* **352**, 91 (2016)
DOI: 10.1126/science.aad0467

This PDF file includes:

Materials and Methods

Methods summary

Lnc13 and coding gene expression levels were quantified by RT-QPCR, starting from DNAseI (Qiagen) treated RNA using specific primers. In the case of the human small intestinal biopsy samples, specific TaqMan assays (Applied Biosystems) and One-Step RT-QPCR were used. All pediatric CeD patients were diagnosed according to the ESPGHAN criteria and all CeD patients had elevated titers of anti-tissue transglutaminase-2 antibodies and displayed characteristic histopathologic abnormalities of the small intestinal mucosa; none of the control patients had any small intestinal disorder and all manifested normal mucosal histology on microscopic examination.

RNA pulldown to identify associated proteins was done as described previously(26) using in vitro transcribed, biotinylated lnc13 and mass spectrometry.

For confirmation of lnc13 binding to Dcp2, we used the RNA IP technique. In vitro transcribed WT or 5' mutant lnc13 was incubated with lysates from cells in which flag-Dcp2 was overexpressed, the complex was pulled-down with a flag antibody against flag-Dcp2. Binding of the different alleles of human lnc13 to hnRNP-D was quantified using total RNA extracted from cells with homozygous genotypes for the distinct alleles or using cells expressing both alleles of lnc13. Amounts of lnc13 bound to immunoprecipitated flag hnRNP-D were quantified by either by regular RT-QPCR or using a dual color allele specific TaqMan assay (Applied Biosystems).

Materials

Oligonucleotides. The complete list of oligonucleotides used for PCR, QPCR, silencing, *in vitro* transcription and cloning is included in the Suplemmentary Information (Supplementary Table 4).

Plasmids. Mouse lnc13 was cloned from mouse cDNA into the pBabe puro vector using BamHI and SalI sites. Mouse Dcp2 was subcloned from pIVT vector kindly provided by

Dr. Richard Schultz. hnRNP-D vectors were previously generated in the lab of Dr. Schneider. shRNA was cloned in the pLKO.1-puro vector following the protocol from Addgene.

Cells. Primary BMDMs were generated by culturing bone marrow from WT and Dcp2/hnRNPD KO C57Bl/6 mice in 20% L929 cell-conditioned medium. For LPS stimulations, cells were seeded in 12-well plates at 10^5 cells/ml and stimulated with 10ng/ml of *E. coli* LPS at different time points.

Macrophages immortalized by inoculation with J2 retrovirus[31] were used for the establishment of a stable lnc13 overexpressing cell line using a pBabe puromycin vector and BamHI and SalI restriction sites and for establishment of the lnc13 knockdown cell line using the lentiviral pLKO.1-puro vector. Immortalized macrophages were also used for silencing experiments accomplished by transfecting 100nM of siRNAs using the HiPerfect reagent (Qiagen); expression was checked 48h post-transfection. siRNAs were designed and ordered from Bioneer. Dcp2 KO macrophages from Rutgers University and Myd88 KO macrophages from UCSF and WT littermate cells for each condition were also immortalized using J2 retrovirus.

Human Dcp2 THP-1 KO and mutant cell lines were generated in Prof. Kiledjians laboratory at Rutgers University. Dcp2 knockout cell lines were generated by CRISPR Cas9 technology using two guide RNAs (gRNAs; 5' UAUCAAAGACUAUAUUUGUA 3' and 5' AACCAGUUUCUUCAAAGACC 3') designed to target the Dcp2 genomic region at the catalytic site. Double stranded DNA oligonucleotides corresponding to the gRNAs were inserted into a modified lentiCRISPR v2 vector (Addgene) where the Cas9 cassette was replaced with the mutant nickase version (Cas9n). Lentiviral particles were packaged in 293T cells for each gRNA and then equally combined to infect THP-1 cells at a MOI of ~10 in the presence of polybrene (8 ug/mL). The infected cells were then subject to puromycin selection for 3 days and viable cells were used for serial dilution to generate single cell clones. The genomic modification was screened by PCR and

sequencing. In Dcp2 knockout line 1 the two alleles were disrupted to generate out-of-frame mutation after T149 and K154, respectively. Line 2 contains two alleles with in-frame deletions in the catalytic Nudix fold region of 8 (F151 to C158) and 12 (E148 to K159) amino acids, respectively. Changes in DCP2 protein expression were confirmed by Western blot.

For the human hnRNPD knockdown, U937 cells were transduced using a MCSV based shRNA expression vector for hnRNPD generated in the laboratory of Prof. Schneider. Gene expression was checked 48h post-infection.

For the RIP experiments, 293FT cells were seeded at 10^6 density and transfected with the Dcp2 and hnRNPD plasmids using Lipofectamine 2000, and lysates were collected after 48h.

Cells homozygous for each of the rs917997 genotypes (CC and TT) were acquired from Coriell Cell repository.

Patient samples. Celiac disease in pediatric patients was diagnosed according to the ESPGHAN (European Society of Pediatric Gastroenterology Hematology and Nutrition) criteria in force at the time of recruitment, including anti-gliadin (AGA), anti-endomysium (EMA) and anti-transglutaminase antibody (TGA) determinations as well as a confirmatory small bowel biopsy. All adult CeD patients had elevated anti-tissue transglutaminase-2 antibody titers and they displayed characteristic small intestinal histopathologic abnormalities, including villous atrophy, crypt hyperplasia and intraeptihelial lymphocytosis. The study was approved by the Institutional Board (Cruces University Hospital code CEIC-E09/10 and Basque Clinical Trials and Ethics Committee code PI2013072) and analyses were performed after informed consent was obtained from all subjects or their parents. Biopsy specimens from the distal duodenum of each patient were obtained during routine diagnosis endoscopy. None of the patients suffered from any other concomitant immunological disease. None of the controls showed small intestinal inflammation at the time of the biopsy.

For lncRNA and gene expression analyses twenty three intestinal biopsies taken from pediatric CeD patients at the time of diagnosis mean age 2.7 years (1.2-9.2); 17 female / 6 male (on gluten-containing diet, positive for CeD-associated antibodies and with atrophy of intestinal villi with crypt hyperplasia) were compared to 23 tissue samples obtained from the same patients in remission after being treated with gluten-free diet (GFD) for more than two years (asymptomatic, antibody negative and with a normalized intestinal epithelium at that time) and 15 control samples (mean age 8.6 years (2.34-14.8); 10 female /5 male) for gene expression evaluation. Paraffin-embedded intestinal sections of 5 adult CeD patients (age 40.8±14.7, 4 males and 1 female) and 5 healthy controls (age 50±14.3, 2 males and 3 females) were used for in situ detection of lnc13. Cytoplasmic and nuclear fractions from three active patients and three healthy controls were used to evaluate Dcp2 localization.

Materials

RACE. Rapid Amplification of cDNA ends (RACE) was performed using the FirstChoice RNA-ligation mediated RACE (RLM-RACE) kit from Ambion to determine the ends of lnc13. For the 5' end total RNA from mouse macrophages was treated with calf intestinal phosphatase (CIP) to remove 5' phosphate from non capped transcripts, resulting in 5' capped transcripts and RNAs with 5' hydroxyl ends. Then, the 5' 7methyl-guansine cap strucruture was removed by tobacco acid pyrophospatase (TAP) resulting 5' mono-phosphate transcript exclusively from intact 5' transcripts. An RNA adaptor with 5' and 3' hydroxyl groups was then ligated to the 5' mono-phospate RNAs. For the 3' RACE cDNA was synthesized using a 3'RACE adapter . RT-PCR using a lnc13 specific primer and a primer binding to the ligated RNA adaptor was performed to amplify the ligated lnc13 followed by TOPO TA cloning and sequencing to determine the very 5' and 3' end sequences of the lncRNA.

Northern blot. For northern blot 10μg of total RNA was collected from cultured macrophages and resolved on 1% agarose-formaldehyde gel. RNA was transferred to a Hybond nylon membrane using the Trans-Blot SD semy-dry electrophorectic transfer (BioRad) Biotin-labeled antisense lnc13 was made using T7 RNA polymerase by IVT with the biotin labeling Kit (Roche). Membrane was pre-hybridized for 1 hour at 42ºC and incubated with the probe overnight at the same temperature. After washing, membrane was blocked and incubated with streptavidin HRP.

DNase hypersensitivity assay. QPCR primers were designed for the DNAse hypersensitivity regions and for random regions within *IL18RAP* and human *lnc13*. Cells were lysed in lysis buffer + NP-40 and nuclei were pelleted and resuspended in nuclei wash buffer. DNaseI was added (Optimum concentration: 11U/million cells) and incubated for 10 min at 37ºC, the reaction was stopped by adding EDTA. The digested DNA was incubated at 55ºC with proteinase K and the DNA was extracted. QPCR was performed on not digested and digested DNA, with the expectation of higher differences in amplification in the regions in which DNaseI cuts. This method was adapted from a previously described protocol[32].

Quantification of molecules per cell. In order to determine the copy number of lnc13 in human U937 cells, a reference plasmid was generated incorporating the cDNA sequence of lnc13 in a PCR blunt vector. Absolute quantification was performed using ten 2-fold serial dilutions of the reference standard. Ct versus the dilution factor was plotted in a base-10 semi-logarithmic graph, fitting the data to a straight line. Plot was then used as a standard curve for extrapolating the number of molecules of lnc13 in the cells.

RNascope technology. *In situ* RNA detection was performed using RNascope technology (Advanced Cell Diagnostics) and a custom probe in formalin fixed small intestinal biopsy following the manufacturer's instructions. *E. Coli* DapB probe was used as a negative and human PPIB as a positive control.

RNA extraction, RT and QPCR. Total RNA was extracted from cells using QIAGEN RNA mini/micro kits. All samples were subjected to DNAse I treatment. A total of 1ug of RNA was used for retrotranscription using SSIII enzyme (Invitrogen) and Real time QPCR was carried out using 2X SYBR green fluorescent dye (Quanta Bioscience). The amplified transcripts were quantifed using the comparative Ct method. All experiments were performed in triplicate.

RNA antisense purification (RAP)

RNA antisense purification was performed following an adapted protocol from the Guttman lab at Caltech. In brief, probes were generated by *in vitro* transcribing biotinylated antisense lnc13 followed by controlled RNA fractionation (Ambion). Sense probes were used as a negative control due to their inhability to bind lnc13. Chromatin extracts from macrophages were prepared after formaldehyde crosslinking and sheared by sonication. Fragmented chromatin was hybridized with control probes, or lnc13-specific RNA probes, captured using MyOne T1 Streptavidin beads (Invitrogen), washed extensively, followed by elution of enriched RNA and DNA. Retrieved RNA and DNA was purified using QIAGEN columns. RNA was converted to cDNA using SSIII (Qiagen). Enrichment of lnc13 and the targets was quantified by QPCR using specific primers (Supplementary Table 4).

***In vitro* transcription and binding partner recognition**. Sense and antisense lnc13 were amplified from mouse cDNA using a T7 promoter primer. The PCR product was purified and used for *in vitro* transcribing biotinylated RNA using the T7 polymerase (Promega) and RNA biotin labeling kit (Pierce). 3ug of purified lnc13 RNA was mixed and incubated with nuclear extracts from $2X10^7$ iBMM. Streptavidin beads were added to the reaction and further incubated. After incubation, beads were washed 5 times[22]. Samples were sent for mass spectrometry and subjected to in-solution digestion followed

by nano LC-MS/MS analysis. The proteins binding exclusively to the sense lnc13 were selected for further analysis.

Lnc13 pulldown. For verification of interactions of lnc13 with Dcp2 and hnRNPD, flag tagged proteins were overexpressed in 293FT cells and lysates were used for the experiments. Flag-Dcp2 lysates were mixed and incubated with IVT WT and 5' mutant forms of lnc13. In the case of hnRNPD, lysates were incubated with whole RNA extracted from six different lymphoblastoid cells lines homozygous for each of the rs91779 (and LD SNPs) genotypes (three cell lines per genotype). Dcp2 and hnRNPD were pulled-down using a flag antibody and protein G beads. Pulled-down RNA was isolated from the beads and amounts of bound lnc13 were assessed by RT-QPCR. In the case of HDAC1 experiments pulldown of endogenous lnc13 was performed using HDAC1 antibody (Santa Cruz Biotechnology) in either mouse or human macrophage cell lines. For endogenous lnc13 pulldown, 293FT and MCF7 lnc13 heterozygous cell lines were transfected with flag-p42 using lipofectamine and Fugene 6 respectively. After 48h cells were lysed and p42 was pulled-down. RNA was isolated from the beads and amounts of each of the alleles were quantified using retrotranscription followed by QPCR using a allele specific TaqMan assay with two different fluorophores.

Cellular fractionation. For quantification of lnc13 levels in nuclear and cytoplasmic compartments, nuclei were isolated using C1 lysis buffer as described previously[23] and amount of specific nuclear RNA measured by RT-QPCR was compared to the total amount of the RNA in the whole cell. Nuclear/cytoplasmic protein fractionation was done using hypotonic and hypertonic buffers with NP-40 detergent. For cytoplasm, nucleoplasm, chromatin fractionation, we followed a protocol from the Mostolovski lab. Briefly, hypotonic buffer, low salt buffer and 0.2N HCl were used respectively for each fraction. Cells were crosslinked before fractionation. Both RNA and proteins were extracted from fractions. Cellular fractionation of intestinal biopsies was done using a nuclear extract kit (Active Motif) following manufacturer's instructions

Western blot. SDS sample buffer was added to cell lysates. Proteins were separated in 10% SDS-polyacrylamide gel and transferred to PVDF membranes. Immunoblotting was performed with the following primary antibodies: antiserum Dcp2 (from Dr. Kiledjian lab), anti-beta tubulin (Sigma Aldrich), anti-Hdac1 (Santa Cruz Biotechnology), anti-H3 (Upstate) , anti-Flag M2 (Sigma Aldrich). Signals were detected using Pierce ECL Western Blotting Substrate (Thermo Scientific).

Chromatin Immunoprecipitation: Mouse and human macrophages were stimulated for four hours. After stimulation cells were fixed with 1% formaldehyde. Cells were lysed for 10 min using hypertonic buffer and nuclei were pelleted and resuspended in RIPA buffer. Chromatin was sheared by sonication and centrifuged to pellet debris. Immunoprecipitations were carried out overnight using protein A magnetic dynabeads (Life Technologies) and 2ug of the Hdac1 antibody (Santa Cruz Biotechnology) or 5ug of the hnRNPD antibody (Millipore). Immune complexes were extracted in 1XTE containing 2%SDS. Protein-DNA crosslinks were reverted by heating at 62ºC for 2 hours. DNA was purified using a QIAGEN kit.

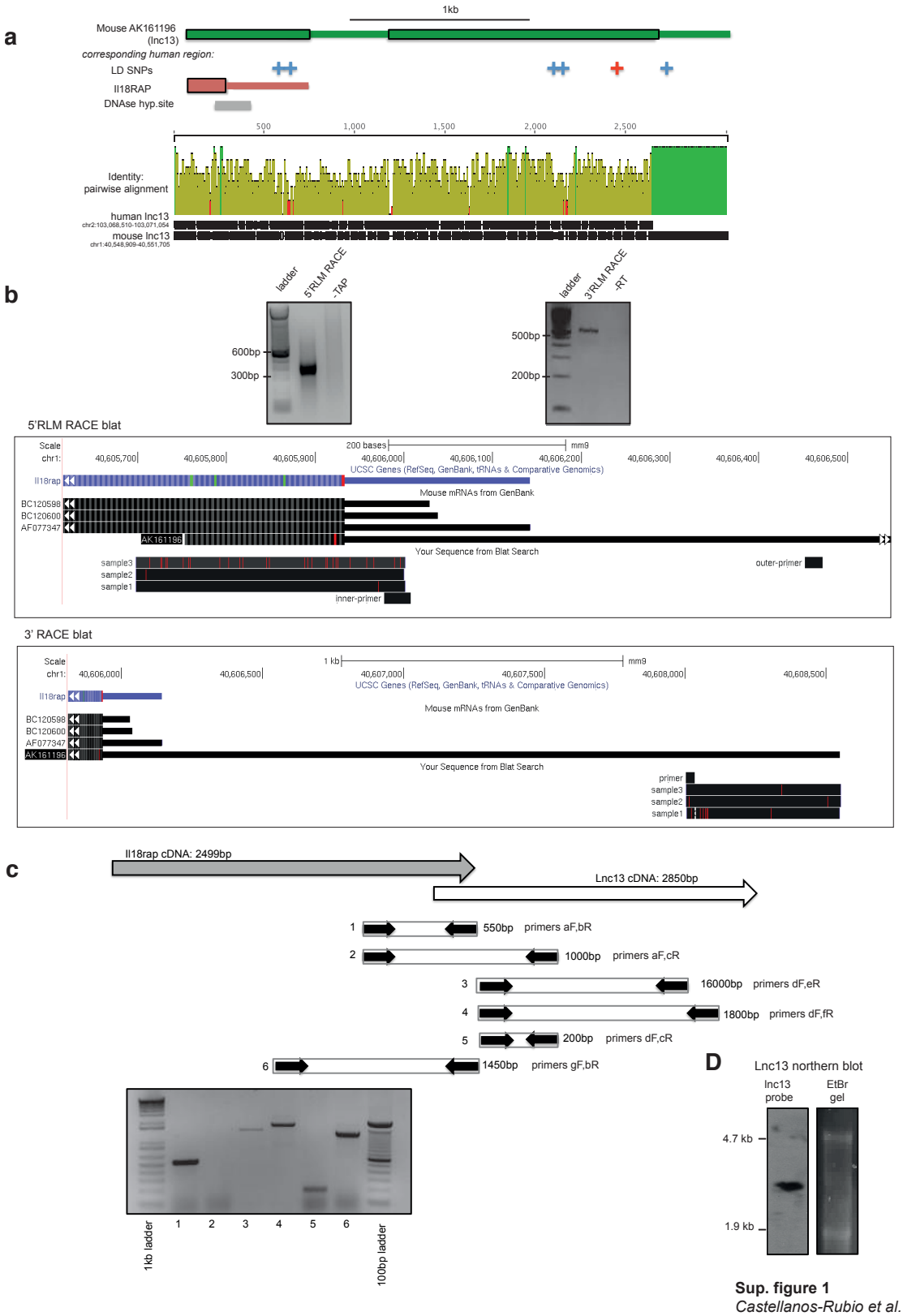

Sup. figure 1
Castellanos-Rubio et al.

Fig. S1. Characterization of mouse AK161196 (lnc13).

a) The information presented was retrieved from the UCSC browser. Human lnc13 genomic location is predicted based on homology with mouse lnc13 (TransMap alignment 66.5% identity). Conserved regions are represented as thicker lines on mouse lnc13 (AK161196). The blue + marks correspond to identified SNPs transmitted as a haplotype block (LD - linkage disequilibrium); rs917997, red + mark, in particular was associated with CeD by GWAS. The grey line indicates DNase hypersensitivity cluster (top). Mouse and human sequences were compared by progressive pairwise alignment (pairwise identity 59%) using the Geneious software (bottom) **b)** 5'RLM-RACE and 3'RACE were performed using the RLM-RACE kit (Ambion) to determine the 5' and 3' ends of lnc13 transcript. PCR bands (top panel) were cloned, sequenced and blated against the mouse genome using the UCSC genome browser (bottom panel). AK161196 (in a black box) is the annotated mouse lnc13. The primers used for the RACE are also aligned against the region. **c)** PCR reactions were carried out using primer pairs that span different regions of IL-18rap, lnc13, and a putative IL-18rap+lnc13 transcript. While PCR primer pairs that span different regions of Il-18rap and lnc13 cDNAs yield predicted amplification products, primer pair that encompass a putative IL18rap+lnc13 transcript, yield no PCR product yield predicted amplification products, primer pair that encompass a putative IL18rap+lnc13 transcript, yield no PCR product. **d)** Northern blot of lnc13 expression in iBMM cells. 10μg of total RNA was run in agarose/formaldehyde gels; after transfer to nylon membranes, lnc13 was detected using antisense biotinylated probe. Ethidium bromide staining of the gel is shown on the right panel.

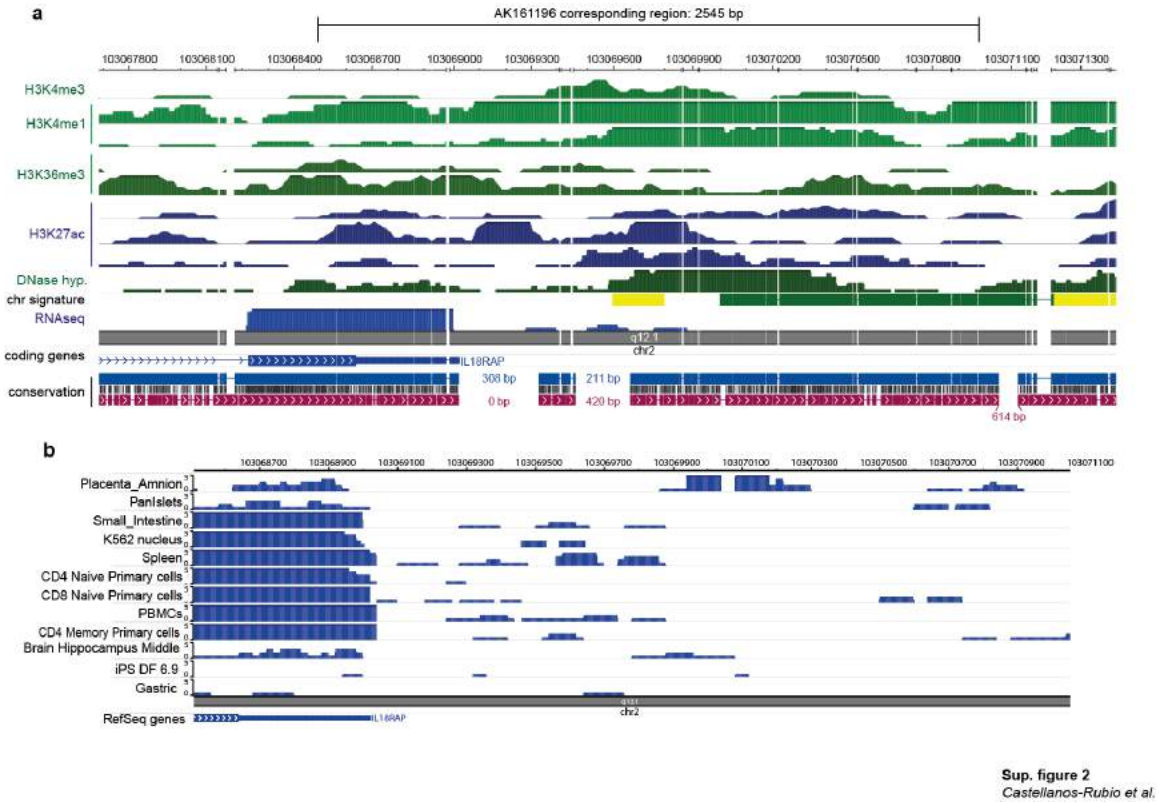

Fig. S2: Data retrieved from the Epigenome Roadmap project.

a) Data from small intestine sample showing the human region corresponding to mouse lnc13 (AK161196); H3K4me3, H3K4me1, H3K27ac and H3K36me3 peaks denote areas actively transcribed. The chromatin signature points to enhancers (yellow) and actively transcribed chromatin (green). The region encompassing lnc13 is indicated by the line designated as AK161146. **b)** RNAseq signals in different tissues also point to the existence of a transcribed region.

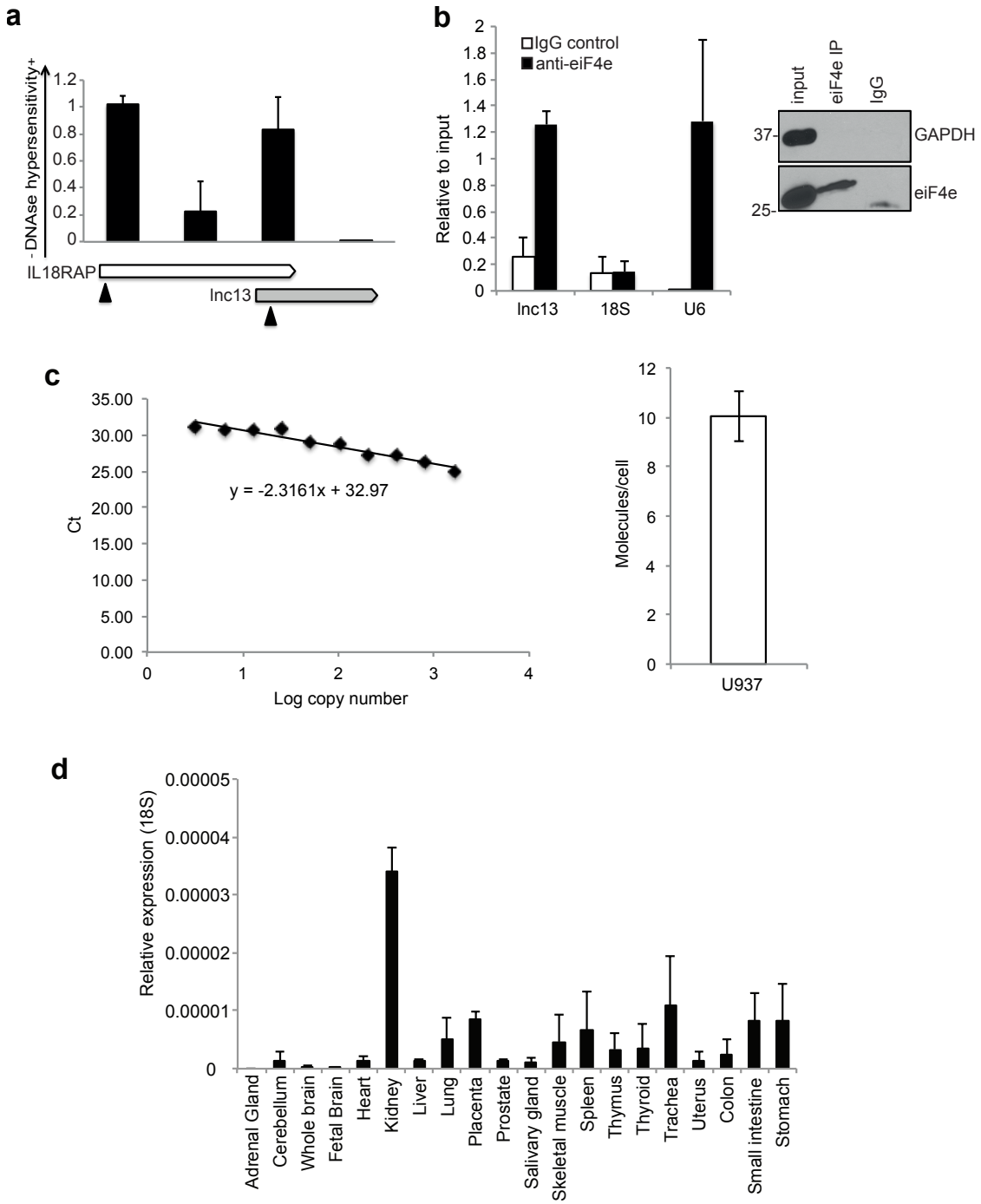

Sup. figure 3
Castellanos-Rubio et al.

Fig. S3: Characterization of human lnc13.

a) DNase hypersensitivity assessed by quantitative PCR after comparison of non-DNaseI treated and optimal DNAseI treated DNA extracted from human macrophage cell line. White bar corresponds to IL18RAP coding gene, grey bar corresponds to lnc13. Black arrows point the DNAse hypersensitivity sites as described by ENCODE (n=3; average±s.d). **b)** Human lnc13 from U937 cell line immunoprecipitated with the cap binding protein eiF4e. 18S: uncapped negative control; U6 capped positive control. Values were calculated relative to input and are shown as the average and standard error of three independent experiments. **c)** Average molecules per cell in the human U937 cell line (left) calculated using a quantitative approach (right) (average±s.e; n=3). **d)** Lnc13 expression (2-ΔCt) measured by RT-QPCR in RNA pool of different tissues purchased from Clontech (Human total RNA master panel II) (average±s.d; three independent RT-QPCRs) .

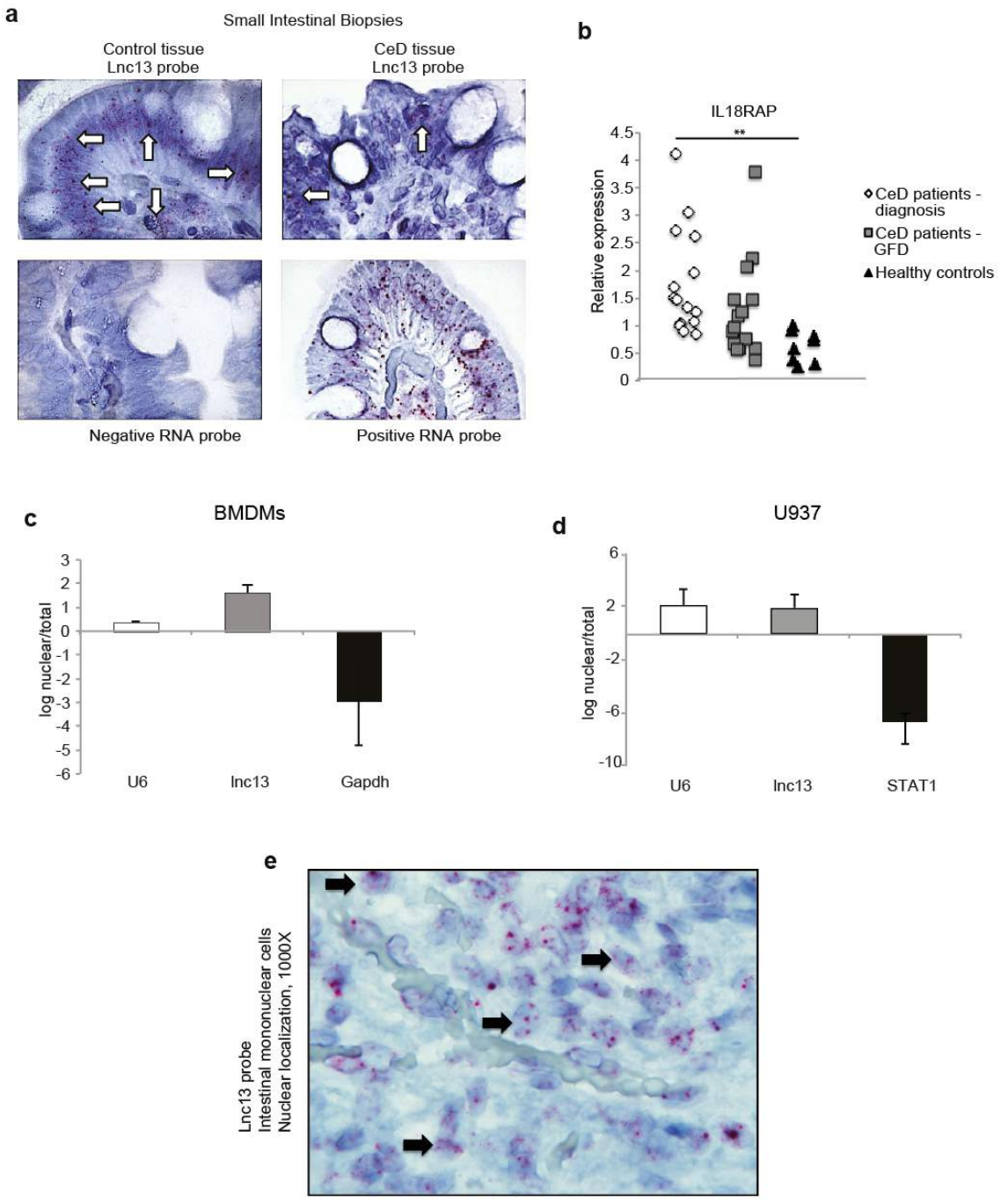

Sup. figure 4
Castellanos-Rubio et al.

Fig. S4: Expression and localization analysis of lnc13.

a) Lnc13 expression in human intestine detected by RNAscope technology. Red dots correspond to lnc13 signal. Positive control: PPIB; negative control: bacterial DapB. Celiac disease samples show disturbed characteristic villous atrophy. Representatitive pictures of five samples per condition. **b)** Expression levels ($2^{-\Delta Ct}$) of the coding gene *IL18RAP* in small intestinal biopsy samples of controls and celiac disease patients; **p<0.01, unpaired t-test. RT-QPCR analysis on whole cell and nuclear RNA to determine localization of lnc13 in **c)** BMDM and **d)** U937 cells. (average±s.d, n=3). **e)** In situ hybridization using RNAscope for lnc13 RNA on a small intestinal (duodenal) biopsy from a celiac disease patient on gluten free diet shows numerous mononuclear cells in the lamina propria that display multiple nuclear lnc13 signals. Picture was taken using 1000X magnification, these were take using a 100X objective magnification (oil immersion) and 10X ocular magnification for a total of 1000X magnification.

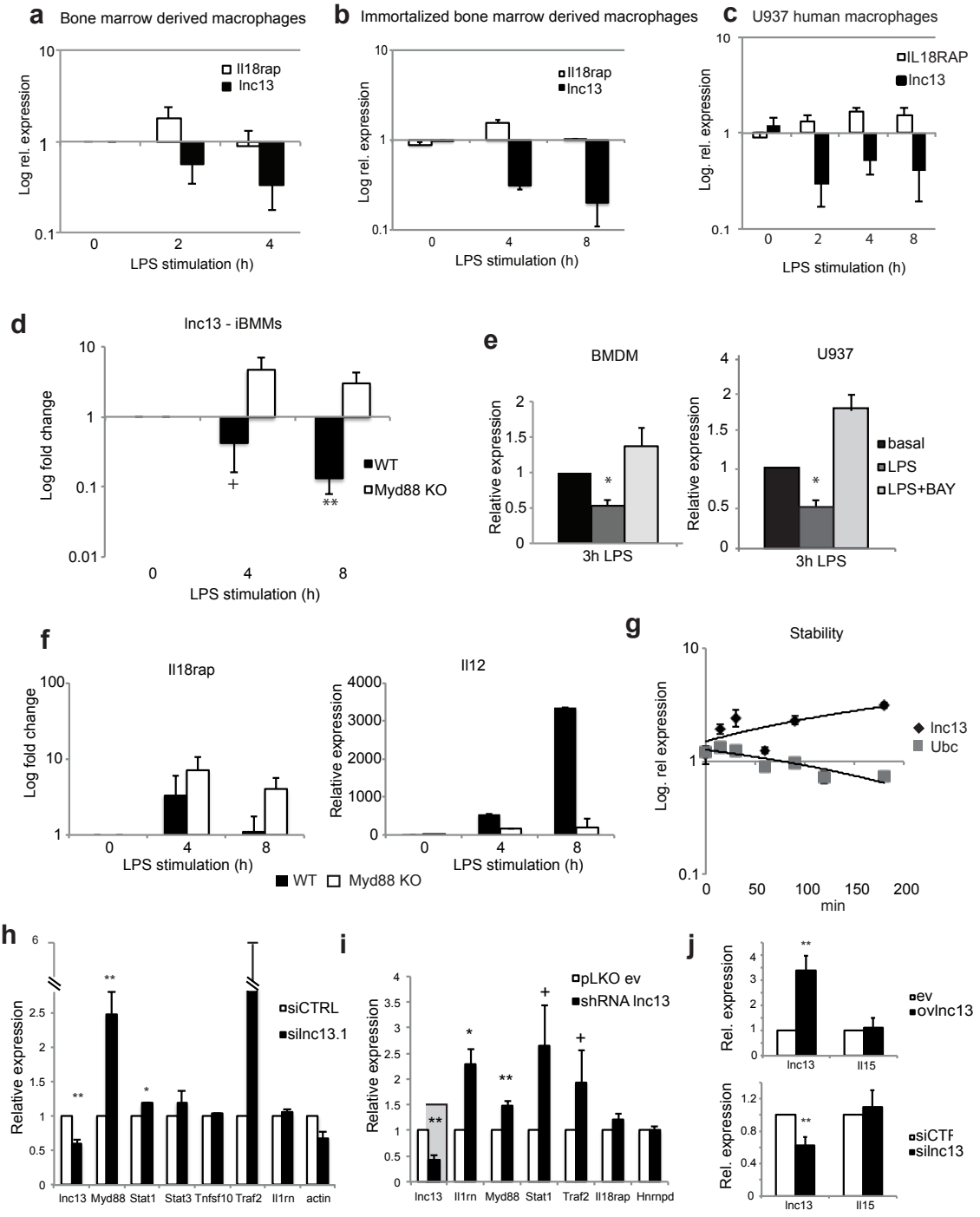

Sup. figure 5
Castellanos-Rubio et al.

Fig. S5: Lnc13 is a NF-kB dependent stable lncRNA that regulates a subset of inflammatory genes.

Lnc13 and Il18rap expression patterns on a time course LPS stimulation of **a)** BMDMs, **b)** immortalized bone marrow derived macrophages, and **c)** human U937 macrophage cell line confirm independent expression of these two transcripts.**d)** LPS induced modulation of lnc13 in WT and Myd88 KO immortalized mouse macrophages. Data represents the average and standard deviation of three independent experiments. **p<0.01, +p<0.1, based on an unpaired t-test. **e)** LPS induced lnc13 downregulation is blocked after NF-κB inhibition by BAY-11-7082 in mouse (left) and human (right) macrophages. RT-QPCR data is represented as the average +/- standard error of three independent experiments. p-values were calculated relative to basal level, *p<0.05, **p<0.01 based on unpaired t-test **f)** LPS induced modulation of Il18rap (left) and Il12 (right) levels in WT and Myd88 KO immortalized mouse macrophages. Data represents the average and standard error of three independent experiments. **g)** Stability of lnc13 measured by QPCR in cells treated with actinomycin (inhibitor of transcription) for a 3h time period. Data is represented as the average and standard error of three independent experiments. Ubc is used as a short half-life mRNA control. **h)** Silencing, using custom siRNA and HiPerfect reagent in immortalized macrophages, of lnc13 influences the expression of coexpressed genes in mouse macrophages. Data represents the average and standard error of three independent experiments. **p<0.01, *p<0.05. **i)** Stable knockdown of lnc13 using a shRNA and pLKO.1-puro lentiviral plasmid. 60% decrease in lnc13 levels (box inlet) cause at least 50% increase in target genes. Data represents the average and standard error of three independent experiments; **p<0.01, *p<0.05, +p=0.1 based on unpaired t-test. **j)** Effect of lnc13 overexpression (top) and silencing (bottom) in the celiac disease related Il-15 gene. Data represents the average and standard error of three independent experiments; **p<0.01, based on unpaired t-test.

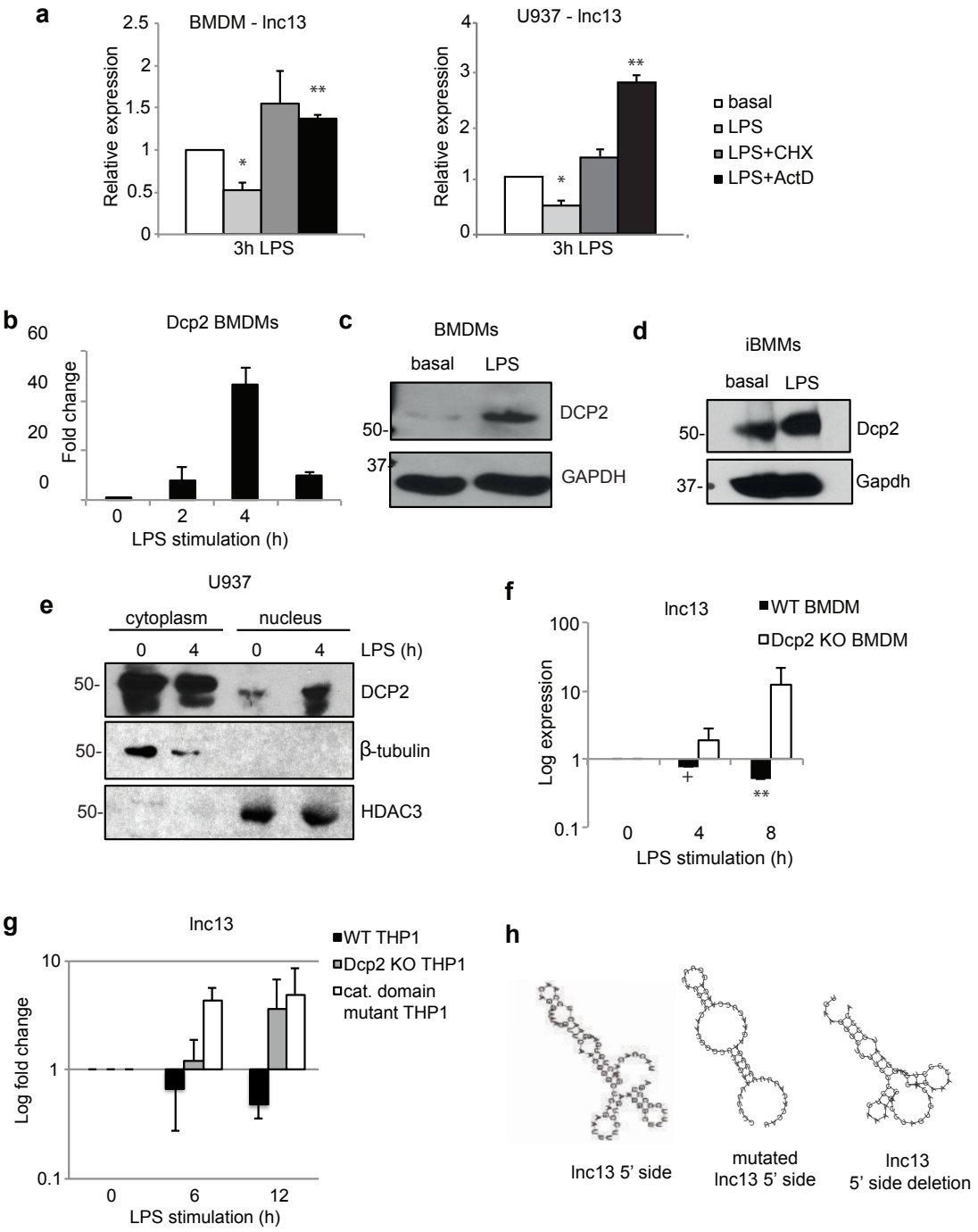

Sup. figure 6
Castellanos-Rubio et al.

Fig. S6: Decapping enzyme 2 regulates lnc13 levels.

a) LPS induced lnc13 downregulation is transcription (ActD; transcription inhibitor) and translation (CHX: protein synthesis inhibitor) dependent in BMDMs (left) and human U937 cells (right). RT-QPCR data is represented as the average +/- standard error of three independent experiments. p-values were calculated relative to basal level, *$p<0.05$, **$p<0.01$ based on unpaired t-test. **b)** Dcp2 expression was measured by RT-QPCR in response to LPS stimulation in BMDMs. Data represents the average and standard error of three independent experiments. Total Dcp2 levels are increased after LPS stimulation in **c)** BMDMs and **d)** iBMMs. **e)** Dcp2 levels are increased in the nucleus after LPS stimulation in human U937 cells. **f)** Lnc13 expression pattern after LPS stimulation of WT (black bars) and Dcp2 KO (white bars) bone marrow derived macrophages. Data represents the average and standard error of three independent experiments. **$p<0.01$, +$p<0.1$, based on an unpaired t-test. **g)** Lnc13 expression pattern after LPS stimulation in human THP-1 cell lines. WT cells (black bars), Dcp2 KO cells (grey bars) and mutant cells for the catalytic domain of Dcp2. Data represents the average and standard error of two independent experiments. **h)** The secondary structure of the 5' loops of wildtype and mutated forms of lnc13 were predicted using the Vienna package.

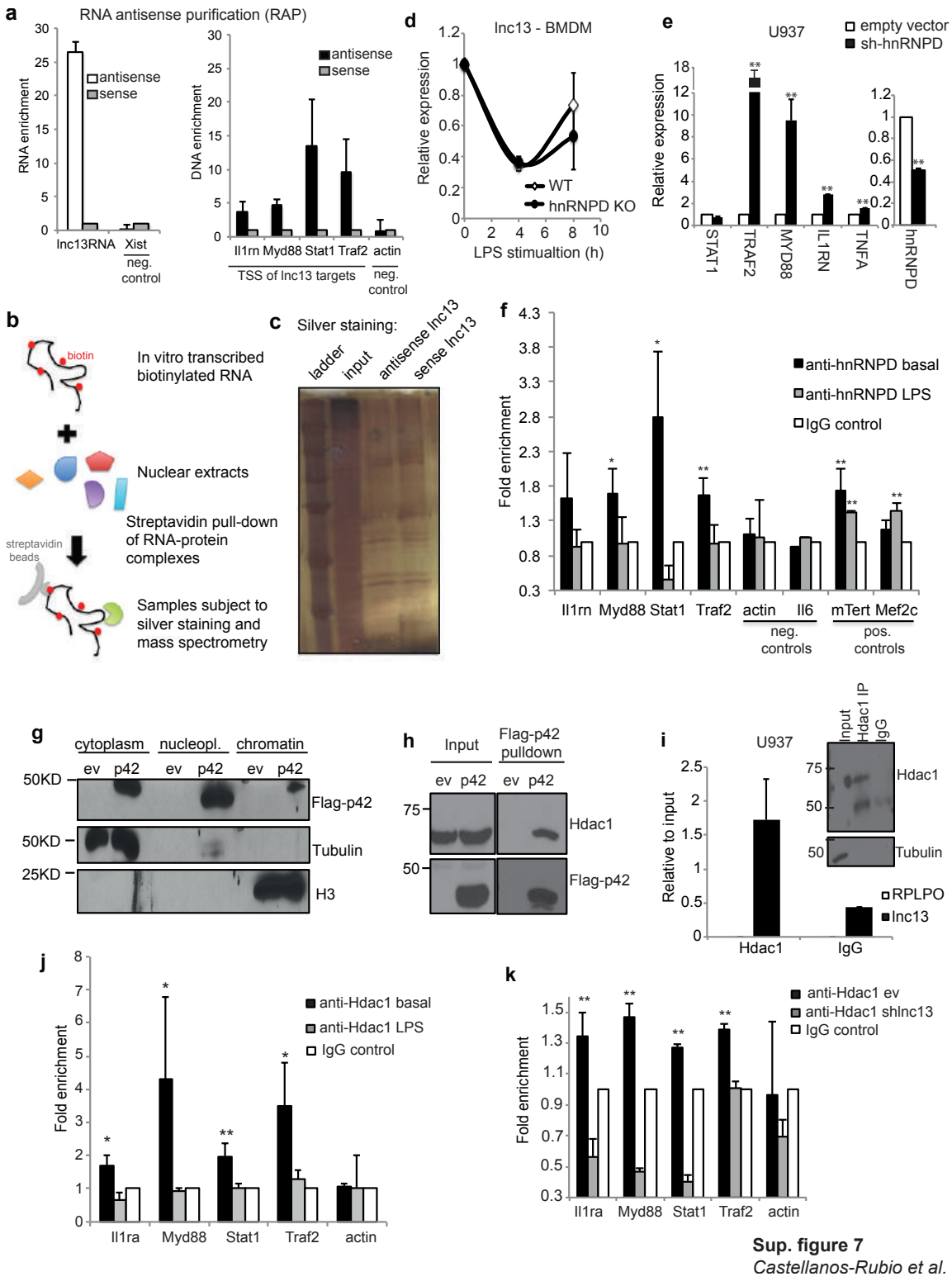

Sup. figure 7
Castellanos-Rubio et al.

Fig. S7: Lnc13 regulates gene expression by chromatin binding.

a) Lnc13 and Xist (chromatin bound lncRNA) RNA enrichment (left) and target gene TSS site DNA enrichment using an independent set of primers (right) after RNA antisense purification of lnc13. Data represents the average and standard error of three experimental replicates.**b)** Flowchart of the strategy for identification of lnc13-binding partners. Sense and antisense *in vitro* transcribed biotinylated lnc13 were incubated with nuclear extracts from mouse macrophages. Streptavidin beads were used to pulldown the RNA-protein complexes. The samples were evaluated by mass spectrometry, and **c)** the protein band pattern bound to each of the RNAs was concurrently visualized by silver staining. A representative image of three independent experiments is shown. **d)** Lnc13 fold change after LPS stimulation in BMDMs isolated from three WT and three hnRNPD KO mice. Data represents average and standard error. **e)** Target gene expression in cells knockdown for hnRNPD measured by RT-QPCR. Data represents average and standard error of three quantifications; *$p<0.05$, **$p<0.01$. **f)** ChIP of hnRNPD shows enrichment around TSS of lnc13-regulated genes in unstimulated immortalized mouse macrophages when compared with LPS stimulated cells (with lower levels of lnc13). Data represents the average fold enrichment and standard error of three independent experiments. Actin and Il6 were used as a negative IP control, mTert and Mef2c were used as positive IP controls. *$p<0.05$, **$p<0.01$. **g)** Flag p42 is also localized in the chromatin fraction. **h)** Hdac1 is detected together with the p42-lnc13 complex in the flag p42 RNA IP. Blot representative of four independent pulldowns. **i)** Hdac1 is able to retrieve endogenous lnc13 in human U937 cells. Lnc13 levels assesed by RT-QPCR after RNA IP (left) (average and standard error of three independent experiments) and WB showing nuclear Hdac1 IP (right). **j)** ChIP of Hdac1 shows enrichment around TSS of lnc13 regulated genes in unstimulated mouse macrophages when compared with LPS stimulated cells. Data represents the average fold enrichment and standard error of three independent

experiments. Actin was used as a negative IP control. *p<0.05, **p<0.01 based on one-tail z-test. **k)** ChIP of Hdac1 in empty vector (ev) and lnc13 shRNA transduced macrophages shows loss of Hdac1 binding to the TSS the target genes in the absence of lnc13. Data represents the average fold enrichment and standard error of three experimental replicates. Actin was used as a negative IP control. **p<0.01 based on one-tail z-test.

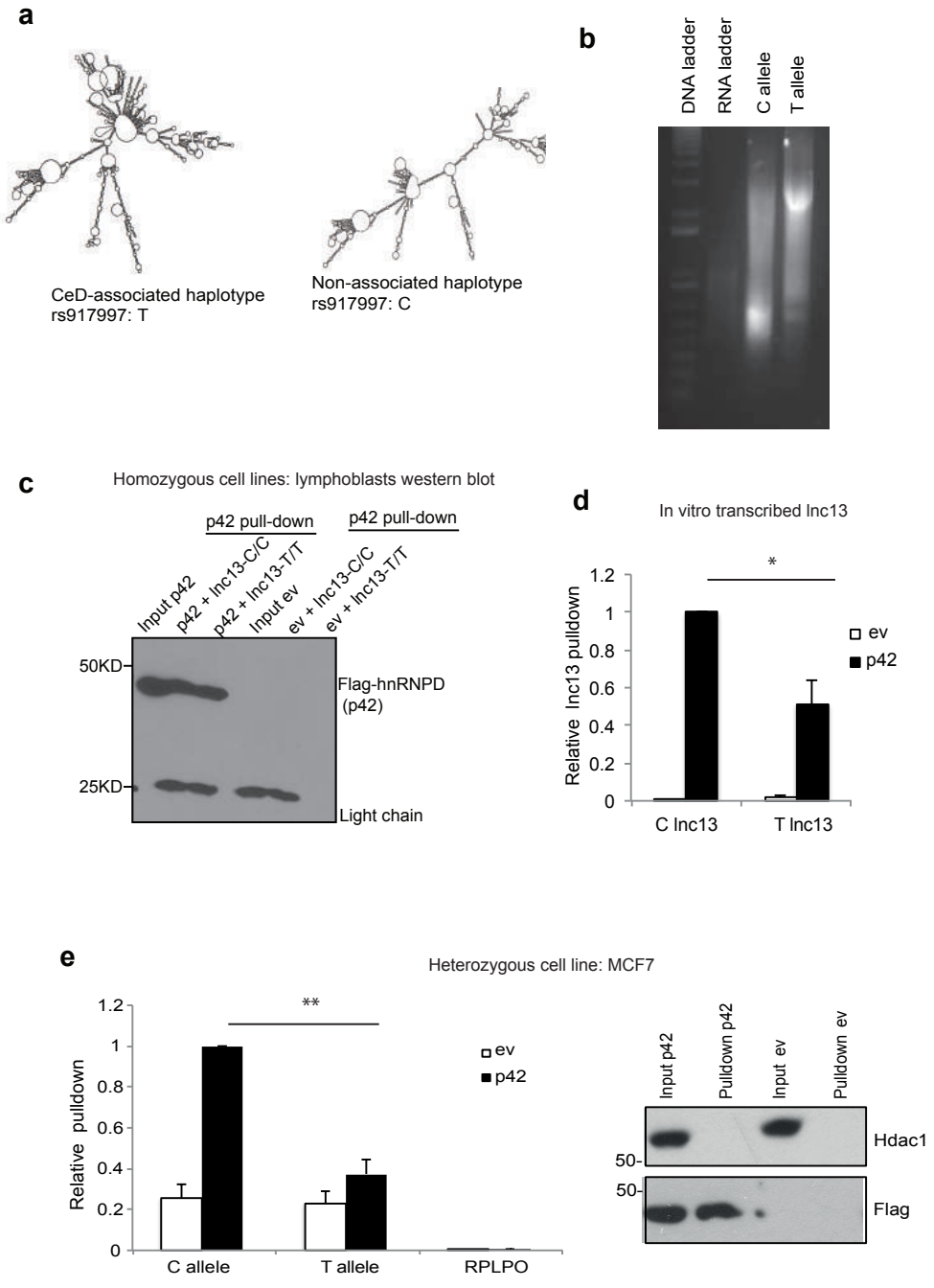

Sup. figure 8
Castellanos-Rubio et al.

Fig. S8: Lnc13 binds hnRNPD in a disease-associated genotype-dependent manner.

a). Predicted secondary structure of human lnc13 variants (Vienna package), 5 SNPs in linkage disequilibrium with the CeD associated rs917997. T: risk allele as assesed by GWAS. **b)** Differential mobility of in vitro transcribed (IVT) lnc13 alleles in a non-denaturing agarose gel. **c)** Total RNA extracted from cells expressing different lnc13 variants was incubated with lysates of cells overexpressing flag-hnRNPD, and relative binding affinity relative to the CC lnc13 was assessed by flag immunoprecipitation and subsequent RT-QPCR analysis. Representative blot of the pulldown. **d)** IVT C allele is retrieved more efficiently than the risk T allele by flag-p42 pulldown. Data is represented as the average and standard error of three independent experiments. C allele pulldown values were considered as 1. *$p<0.05$ based on paired t-test. **e)** Heterozygous cell line MCF7 (breast cancer) was transfected with a flag-hnRNPD and after immunoprecipitation endogenous amount of each allele was quantified by a dual fluorescence TaqMan assay. Retrieved lnc13 was normalized to input and and pulldown values were calculated relative to C allele. Data represents the average and standard error of 3 independent experiments. **$p<0.01$ based on paired t-test.

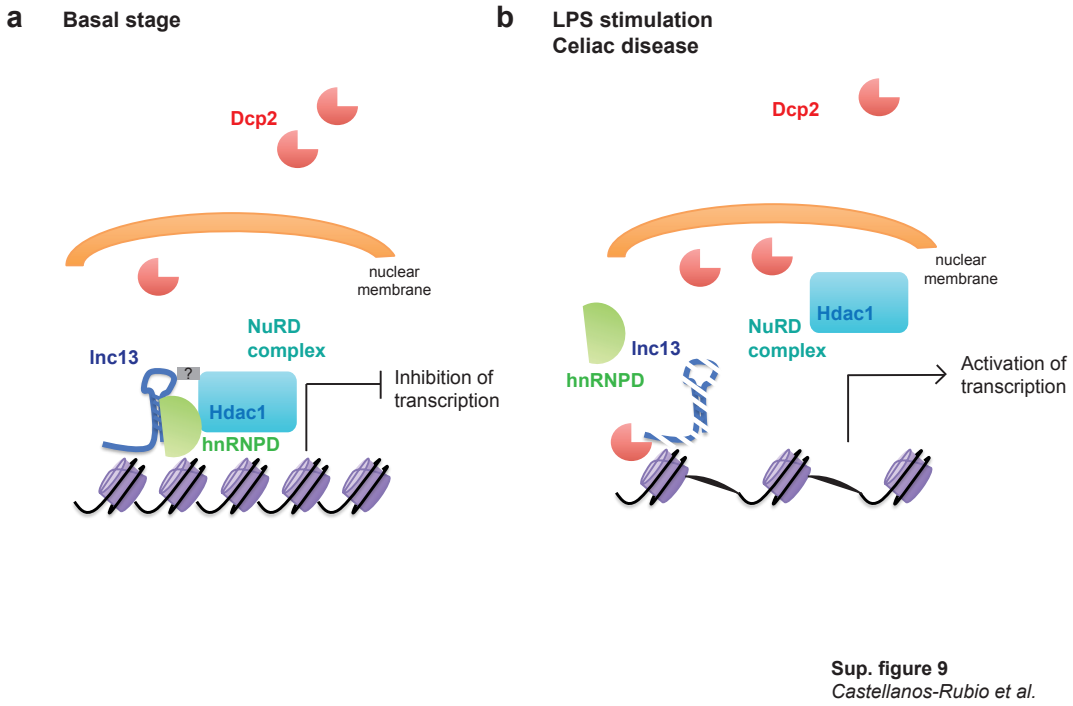

Sup. figure 9
Castellanos-Rubio et al.

Fig. S9: Schematic representation of the lnc13 mechanism of action.

a) At basal stage lnc13 and associated proteins are bound to chromatin inhibiting the expression of inflammatory genes. **b)** In celiac disease condition or response to LPS (NF-κB activation), Dcp2 is translocated to the nucleus degrading lnc13 that releases the complex and permits inflammatory gene expression.

chr	rsID	Distance	Coding gene
1	rs2816316	465	RGS1
2	rs917997	1542	IL18RAP
1	rs10903122	6219	RUNX3
1	rs12727642	1106	PARK7
1	rs859637	34045	FASLG
1	rs296547	7273	C1orf106
6	rs2327832	21582	OLIG3
3	rs13314993	17627	CCR4
6	rs1033180	8192	IRF4
X	rs5979785	21702	LOC349408
8	rs9792269	31539	MIR1208
14	rs4899260	15013	ZFP36L1
3	rs6441961	42840	CCR2
4	rs6822844	24361	IL21

Sup. table 1
Castellanos-Rubio et al.

Table S1: SNPs located in intergenic regions that have been associated with CeD in GWAS as retrieved by the Haploreg online tool(9). Distance corresponds to base pairs to the closest coding gene.

	LPS (h)				
	2	4	8	16	R-value
Sele	-28.52	-30.23	-32.24	-34.20	0.76
Tlr4	-2.22	-1.14	-2.18	-1.14	0.79
Myc	-2.08	-0.60	-1.24	-2.21	0.45
F8	-0.51	-0.18	0.53	-0.36	0.51
Nqo1	-0.17	0.09	0.43	1.45	0.32
Ccnd1	-1.35	-2.76	-3.24	-4.21	0.77
Plau	-0.88	-2.15	-3.17	-4.14	0.96
Ncoa3	-0.73	-0.22	-1.15	-2.12	0.98
Il1r2	0.21	-1.11	-1.23	-2.23	0.81
Map2k6	-0.65	-2.88	-2.24	-0.21	0.89
Smad3	-0.11	30.49	-0.38	-0.51	0.36
Ccr5	-0.31	0.59	0.77	0.78	0.03
Ikbkg	-0.55	0.42	1.44	-0.57	0.88
C4	-0.37	0.40	1.46	0.45	0.36
Ikbkb	-0.37	0.19	0.77	-0.23	0.77
Selp	0.92	1.93	3.52	0.55	0.44
Xiap	-0.16	0.52	-0.20	-1.23	0.59
Bcl2l1	0.57	0.42	0.43	-0.55	0.52
Nfkb1	2.74	3.65	2.80	1.80	0.30
Ikbke	2.91	3.91	4.75	3.77	0.45
Tnfrsf1b	3.82	4.72	5.73	4.72	0.85
Birc3	3.85	4.65	3.79	3.81	0.84
Nfkbia	4.06	4.07	4.08	3.07	0.64
Nfkb2	4.27	5.23	5.78	4.78	0.58
Fas	4.66	5.81	5.31	4.28	0.79
Tnfaip3	5.29	5.37	5.39	3.37	0.65
Lta	5.32	6.95	7.77	6.77	0.51
C3	5.49	7.97	7.78	6.77	0.83
Icam1	5.73	5.67	4.33	3.34	0.78
Ptgs2	5.95	8.64	8.56	8.52	0.36
Tnf	6.96	7.82	6.80	4.81	0.84
Ccl22	7.35	8.46	8.46	6.48	0.50
Vcam1	7.84	7.98	6.99	4.97	0.66
Ccl5	7.86	10.04	10.79	10.81	0.45
Cxcl10	8.69	9.85	6.80	5.80	0.85
Cxcl9	8.70	10.45	10.78	9.77	0.40
Il1a	10.97	12.91	13.74	14.79	0.77
Cxcl3	11.14	12.67	13.67	13.67	0.84
Il12b	12.03	13.09	12.80	11.80	0.81
Csf2	12.36	12.09	10.79	9.80	0.69
Cxcl1	12.55	12.82	11.79	11.78	0.55
Il6	13.01	16.06	14.64	13.62	0.64
Il1b	13.53	15.06	15.81	16.81	0.70

	LPS (h)				
	2	4	8	16	R-value
Nr4a2	0.40	0.66	1.69	0.67	0.80
Cd74	0.79	1.43	0.76	-0.24	0.81
Il15	3.24	5.35	2.86	0.87	0.03
Csf1	4.91	5.23	3.80	1.76	0.15
Csf2rb	0.26	1.14	0.85	1.91	0.21
Mmp9	0.54	2.46	3.15	5.17	0.84
Egfr	0.55	0.63	0.65	1.62	0.94
Sod2	3.08	4.28	5.27	5.27	0.79
Cfb	4.97	9.38	11.38	12.38	0.93
Stat3	0.12	1.81	2.70	1.70	0.96
Stat1	0.65	2.54	2.55	2.57	0.90
Myd88	1.27	2.68	2.69	1.70	0.91
Traf2	1.31	2.18	2.78	1.79	0.75
Il1rn	2.32	5.31	6.79	5.81	0.84
Ccl12	3.38	5.43	5.41	3.42	0.95
Il2ra	3.99	5.88	6.64	5.61	0.70
Tnfsf10	4.41	7.82	6.81	4.85	0.86
Csf3	7.98	13.20	15.77	14.76	0.68
Trp53	0.91	0.15	-0.85	-0.82	0.93
Egr2	2.54	0.82	0.79	-0.16	0.78
Pdgfb	2.71	1.83	1.29	0.30	0.28
Irf1	4.78	4.56	3.38	2.39	0.09
Adm	5.81	3.13	3.40	3.40	0.28
Cd83	6.53	4.92	3.94	0.95	0.31
Ifnb1	10.71	9.15	5.77	3.77	0.00
Cd80	1.72	1.96	0.41	0.38	0.09
Cdkn1a	1.90	2.49	0.78	0.79	0.14
Birc2	2.10	2.31	0.80	0.78	0.04
F3	3.26	4.15	1.77	1.80	0.01
Rel	3.59	4.05	1.78	1.80	0.18
Rela	1.34	1.46	1.76	0.78	0.14
Mitf	1.84	2.12	2.46	1.45	0.54
Ltb	3.35	3.12	3.78	1.78	0.65
Relb	4.09	3.98	4.98	2.97	0.49
Gadd45b	4.41	4.39	4.78	2.80	0.63
Cd40	6.29	8.12	7.76	4.79	0.53
Lnc13	-1.47	-3.36	-6.07	-6.16	

Sup. table 2
Castellanos-Rubio et al.

Table S2: List of coding genes whose expression was checked for lnc13 target analysis clustered by expression pattern after LPS stimulation. Log 2 fold change values retrieved from the STEM (short term expression miner) software(17). R-values represent the correlation between lnc13 expression and each of the target genes.

Protein name	gi number	Gene name
heterogeneous nuclear ribonucleoprotein A3 isoform b [Mus musculus]	gi|31559916	Hnrnpa3
plectin 1 isoform 1 [Mus musculus]	gi|41322904	Plec1
keratin 15 [Mus musculus]	gi|6680602	Krt15
poly(rC) binding protein 2 [Mus musculus]	gi|6997239	Pcbp2
PREDICTED: p30 DBC protein [Mus musculus]	gi|94397239	NET35
actin related protein 2/3 complex, subunit 5 [Mus musculus]	gi|13385866	Arpc5
splicing factor, arginine/serine rich 9 [Mus musculus]	gi|13385016	Srsf9
PREDICTED: similar to SRp40-1 [Mus musculus]	gi|82895195	LOC675606
peripherin [Mus musculus]	gi|7305413	Prph
myosin XV isoform 1 [Mus musculus]	gi|6754780	Myo15
serine/arginine repetitive matrix 1 [Mus musculus]	gi|7949115	Srrm2
U1 small nuclear ribonucleoprotein 70 kDa [Mus musculus]	gi|67846113	Snrnp70
nuclear receptor coactivator 5 [Mus musculus]	gi|21450271	Ncoa5
heterogeneous nuclear ribonucleoprotein D isoform a [Mus musculus]	gi|116256512	Hnrnpd
inner membrane protein, mitochondrial [Mus musculus]	gi|70608131	Immt
PREDICTED: Crm, cramped-like isoform 1 [Mus musculus]	gi|51770109	CRAMP1L
ribosomal protein L14 [Mus musculus]	gi|13385472	Rpl14
ribosomal protein L23 [Mus musculus]	gi|12584986	Rpl23
LUC7-like 2 [Mus musculus]	gi|20373167	Luc7l
splicing factor 3a, subunit 2 [Mus musculus]	gi|10800150	Sf3a1

Sup. table 3
Castellanos-Rubio et al.

Table S3: List of proteins that specifically bind biotinylated sense lnc13 as assessed by mass spectrometry analysis.

Mouse QPCR primers			
lnc13-F1	ACTGAGCTCCCAAGCATTTG	lnc13-R1	CATGGACTGGCTATTTCTGC
lnc13-F2	GTTTGCAAGACTTTGGCTGAG	lnc13-R2	AGATGGTGCAGCCAGAAAAC
lnc13-F3	AACCAAATGAGGTCCACAGG	lnc13-R3	GGTTAGTGCCAAAGCCAAAG
lnc13-F4	TCCCCTGAGAACCAAATGAG	lnc13-R4	GGTTAGTGCCAAAGCCAAAG
Stat1-F	TCACAGTGGTTCGAGCTTCAG	Stat1-R	GCAAACGAGACATCATAGGCA
Myd88-F	AGGACAAACGCCGGAACTTTT	Myd88-R	GCCGATAGTCTGTCTGTTCTAGT
Tnfsf10-F	ATGGTGATTTGCATAGTGCTCC	Tnfsf10-R	GCAAGCAGGGTCTGTTCAAGA
Il2ra-F	AACCATAGTACCCAGTTGTCGG	Il2ra-R	TCCTAAGCAACGCATATAGACCA
Stat3-F	CAATACCATTGACCTGCCGAT	Stat3-R	GAGCGACTCAAACTGCCCT
Traf2-F	AGAGAGTAGTTCGGCCTTTCC	Traf2-R	GTGCATCCATCATTGGGACAG
Il1ra-F	GCTCATTGCTGGGTACTTACAA	Il1ra-R	CCAGACTTGGCACAAGACAGG
Il15-F	CATCCATCTCGTGCTACTTGTG	Il15-R	GCCTCTGTTTTAGGGAGACCT
Il6-F	TTGCGATGCTAAAGGACG	Il6-R	TGTGGAGAAGGAGTTCATAGC
Hprt-F	GTT AAG CAG TAC AGC CCC AAA	Hprt-R	AGG GCA TAT CCA ACA ACA AAC TT
Il18rap-F	AGACTACTTCCTGAGCACAAGA	Il18rap-R	TGTCCTTACCAATGGTTCTCACT
Dcp2-F	AGACAATGCGATCCGAGTGTG	Dcp2-R	CGTAAGTCGGGACTCCCATTT
Human QPCR primers			
lnc13-F1	AAGGATCATTGCAGGGTCTC	lnc13-R1	GTGGCCAAAAGAAGTCTGAGTC
lnc13-F2	CTTTGGCACCAAGCAACATC	lnc13-R2	TTCACTGAGACCCTGCAATG
RPLPO-F	GCAGCATCTACAACCCTGAAG	RPLPO-R	CACTGGCAACATTGCGGAC
IL18RAP-F	ATGCTCTGTTTGGGCTGGATA	IL18RAP-R	TTAATTCGCTCTCCTGCAACAA
DCP2-F	ATGGAGACCAAACGGGTGGA	DCP2-R	AACCAATGGGCAAGTTCAATCT
cDNA PCRs			
aF	TGCAGATGACATTGTGAGCA	bR	CTTCATTCCACTGCCTGTCA
dF	ACTCCATCTAAAGCCCTTCTGT	cR	GCCAACAACAGATACCATGC
gF	AGACTACTTCCTGAGCACAAGA	eR	CATGGACTGGCTATTTCTGC
		fR	AAAGGTCTGCAGTGTGTCCT
DNAse hypersensitivity			
DHlnc13F	ACGTGGAACCAGCTCAGAAT	DHlnc13R	TCAGCCTGAACACACACACA
DH-IL18RAP-F	TTCAGGTGAGCACAAGTTGC	DH-IL18RAP-R	CCAGGGAAGTGAAACAAAGC
TaqMan assays			
RPLP0-Hs99999902_m1			
TRAF2-Hs00184186_m1			
STAT1-Hs00234829_m1			
MYD88-Hs00182082_m1			
IL1RA-Hs00168392_m1			
Custom lnc13 TaqMan			
Forward Primer	CAGGATCCCTGGCCTTCCT		
Reverse Primer	TGGCCAAAAGAAGTCTGAGTCTT		
Probe	CCGCCACTCTCTGAG		
siRNAs			
siRNA lnc13	UGGUAACCAUGCUUUAUUUtt		
negative control siRNA	CCUACGCCACCAAUUUCGUtt		
Overexpression vector			
Forward	AACTGCATCCTACCACATGCCTGTG	Reverse	AACTGTCGACGAGAAGGAAAGGGT
In vitro transcription			
sense forward	GCTAGTGGTGCTAGCCCCGCGAATTAATACGACTCACTATAGGTACCACATGCCTGTG	sense reverse	GAGAAGGAAAGGGT
antisense forward	GCTAGTGGTGCTAGCCCCGCGAATTAATACGACTCACTATAGGGAGAAGGAAAGGGT	antisense reverse	TACCACATGCCTGTG
mutant lnc13 F	GCTAGTGGTGCTAGCCCCGCGAATTAATACGACTCACTTACCACATTTTTTTGAAGAACTC		
5' deleted lnc13 F	GCTAGTGGTGCTAGCCCCGCGAATTAATACGACTCACTAGGGCTTTTCCCCTGA		
ChIP/RAP primers			
actinproF.mm	GCCTAGTAACCGAGACATTGA	actinproR.mm	AGAAAGCGAGATTGAGGAAG
actinproF2.mm	CGGTTACTAGGCCTGCATTC	actinproR2.mm	GATGCTGACCCTCATCCACT
Il1rnpromF.mm	TCCCATCCCAAGTCATCTTC	Il1rnpromR.mm	GAGAATGGTGGCATTTGAGC
Il1rnpromF2.mm	AGAACCAGTTTGGCTTCTGC	Il1rnpromR2.mm	AGGTTGGTTGCTGATGACTG
Myd88proF.mm	ACGGAAGCCAATCGTAATGC	Myd88proR.mm	AACCTCCTTCCCCAATGTCTAC
Myd88proF2.mm	ACAAAAGTGGGGTGCCTTTG	Myd88proR2.mm	AACTAGGTGTGTTGCCAAGG
Stat1proF.mm	AAGCGGGACAAAAGTTTCGG	Stat1proR.mm	TCAACCAAGCCTGCAAGAAG
Stat1proF2.mm	ATCCGTTCACACGCATGTTC	Stat1proR2.mm	TGGGGAAACTGTCATCGTACAG
Traf2proF.mm	AATTGTGTGGGGATCGAAGGG	Traf2proR.mm	TTTTTCTCGGGATCCTCCACTC
Traf2proF2.mm	ATTTGGTGGCAAGTGACTGC	Traf2proR.mm	AGCAAGGTTGTTGAGGAAGC
mTertproF.mm	CCTCCGCCTACCTAACCTTC	mTertproR2.mm	TTGATGGTCACAATGCTGGT
Il6proF.mm	GTGTGTGTCGTCTGTCATGC	Il6proR.mm	AGGAAGGGGAAAGTGTGCTT
Mef2c-promF.mm	TTAAGTGCCATGACCATCCA	Mef2c-promR.mm	GCACACACTTGCTTCATTTCA

Sup. Table 4
Castellanos- Rubio et al

Table S4: List of oligos used for the different experiments

Author contributions ACR performed the majority of the experiments and helped in writing the paper, RK performed some experiments, NFJ and JRB provided the pediatric CeD patient samples, and analyzed and quantitated the expression of lnc13. GB and PHRG provided adult CeD samples and helped with the RNAscope technology, RS provided AUF1 reagents and knock-outs, MK provided reagents and knock-outs of Dcp2, XL did the Dcp2 CRISPR KO experiments, and SG conceived of the study and wrote the paper.

References and Notes

1. T. Derrien, R. Johnson, G. Bussotti, A. Tanzer, S. Djebali, H. Tilgner, G. Guernec, D. Martin, A. Merkel, D. G. Knowles, J. Lagarde, L. Veeravalli, X. Ruan, Y. Ruan, T. Lassmann, P. Carninci, J. B. Brown, L. Lipovich, J. M. Gonzalez, M. Thomas, C. A. Davis, R. Shiekhattar, T. R. Gingeras, T. J. Hubbard, C. Notredame, J. Harrow, R. Guigó, The GENCODE v7 catalog of human long noncoding RNAs: Analysis of their gene structure, evolution, and expression. *Genome Res.* **22**, 1775–1789 (2012). Medline

2. L. A. Hindorff, P. Sethupathy, H. A. Junkins, E. M. Ramos, J. P. Mehta, F. S. Collins, T. A. Manolio, Potential etiologic and functional implications of genome-wide association loci for human diseases and traits. *Proc. Natl. Acad. Sci. U.S.A.* **106**, 9362–9367 (2009). Medline doi:10.1073/pnas.0903103106

3. G. Jin, J. Sun, S. D. Isaacs, K. E. Wiley, S. T. Kim, L. W. Chu, Z. Zhang, H. Zhao, S. L. Zheng, W. B. Isaacs, J. Xu, Human polymorphisms at long non-coding RNAs (lncRNAs) and association with prostate cancer risk. *Carcinogenesis* **32**, 1655–1659 (2011). Medline doi:10.1093/carcin/bgr187

4. N. Fernandez-Jimenez, A. Castellanos-Rubio, L. Plaza-Izurieta, I. Irastorza, X. Elcoroaristizabal, A. Jauregi-Miguel, T. Lopez-Euba, C. Tutau, M. M. de Pancorbo, J. C. Vitoria, J. R. Bilbao, Coregulation and modulation of NFκB-related genes in celiac disease: Uncovered aspects of gut mucosal inflammation. *Hum. Mol. Genet.* **23**, 1298–1310 (2014). Medline doi:10.1093/hmg/ddt520

5. P. H. Green, C. Cellier, Celiac disease. *N. Engl. J. Med.* **357**, 1731–1743 (2007). Medline doi:10.1056/NEJMra071600

6. P. C. Dubois, G. Trynka, L. Franke, K. A. Hunt, J. Romanos, A. Curtotti, A. Zhernakova, G. A. Heap, R. Adány, A. Aromaa, M. T. Bardella, L. H. van den Berg, N. A. Bockett, E. G. de la Concha, B. Dema, R. S. Fehrmann, M. Fernández-Arquero, S. Fiatal, E. Grandone, P. M. Green, H. J. Groen, R. Gwilliam, R. H. Houwen, S. E. Hunt, K. Kaukinen, D. Kelleher, I. Korponay-Szabo, K. Kurppa, P. MacMathuna, M. Mäki, M. C. Mazzilli, O. T. McCann, M. L. Mearin, C. A. Mein, M. M. Mirza, V. Mistry, B. Mora, K. I. Morley, C. J. Mulder, J. A. Murray, C. Núñez, E. Oosterom, R. A. Ophoff, I. Polanco, L. Peltonen, M. Platteel, A. Rybak, V. Salomaa, J. J. Schweizer, M. P. Sperandeo, G. J. Tack, G. Turner, J. H. Veldink, W. H. Verbeek, R. K. Weersma, V. M. Wolters, E. Urcelay, B. Cukrowska, L. Greco, S. L. Neuhausen, R. McManus, D. Barisani, P. Deloukas, J. C. Barrett, P. Saavalainen, C. Wijmenga, D. A. van Heel, Multiple common variants for celiac disease influencing immune gene expression. *Nat. Genet.* **42**, 295–302 (2010). Medline doi:10.1038/ng.543

7. G. Trynka, K. A. Hunt, N. A. Bockett, J. Romanos, V. Mistry, A. Szperl, S. F. Bakker, M. T. Bardella, L. Bhaw-Rosun, G. Castillejo, E. G. de la Concha, R. C. de Almeida, K. R. Dias, C. C. van Diemen, P. C. Dubois, R. H. Duerr, S. Edkins, L. Franke, K. Fransen, J. Gutierrez, G. A. Heap, B. Hrdlickova, S. Hunt, L. Plaza Izurieta, V. Izzo, L. A. Joosten, C. Langford, M. C. Mazzilli, C. A. Mein, V. Midah, M. Mitrovic, B. Mora, M. Morelli, S. Nutland, C. Núñez, S. Onengut-Gumuscu, K. Pearce, M. Platteel, I. Polanco, S. Potter, C. Ribes-Koninckx, I. Ricaño-Ponce, S. S. Rich, A. Rybak, J. L. Santiago, S. Senapati, A. Sood, H. Szajewska, R. Troncone, J. Varadé, C. Wallace, V. M. Wolters, A. Zhernakova,

B. K. Thelma, B. Cukrowska, E. Urcelay, J. R. Bilbao, M. L. Mearin, D. Barisani, J. C. Barrett, V. Plagnol, P. Deloukas, C. Wijmenga, D. A. van Heel; Spanish Consortium on the Genetics of Coeliac Disease (CEGEC); PreventCD Study Group; Wellcome Trust Case Control Consortium (WTCCC), Dense genotyping identifies and localizes multiple common and rare variant association signals in celiac disease. *Nat. Genet.* **43**, 1193–1201 (2011). Medline doi:10.1038/ng.998

8. D. A. van Heel, L. Franke, K. A. Hunt, R. Gwilliam, A. Zhernakova, M. Inouye, M. C. Wapenaar, M. C. Barnardo, G. Bethel, G. K. Holmes, C. Feighery, D. Jewell, D. Kelleher, P. Kumar, S. Travis, J. R. Walters, D. S. Sanders, P. Howdle, J. Swift, R. J. Playford, W. M. McLaren, M. L. Mearin, C. J. Mulder, R. McManus, R. McGinnis, L. R. Cardon, P. Deloukas, C. Wijmenga, A genome-wide association study for celiac disease identifies risk variants in the region harboring *IL2* and *IL21*. *Nat. Genet.* **39**, 827–829 (2007). Medline doi:10.1038/ng2058

9. L. D. Ward, M. Kellis, HaploReg: A resource for exploring chromatin states, conservation, and regulatory motif alterations within sets of genetically linked variants. *Nucleic Acids Res.* **40**, D930–D934 (2012). Medline doi:10.1093/nar/gkr917

10. P. Carninci, T. Kasukawa, S. Katayama, J. Gough, M. C. Frith, N. Maeda, R. Oyama, T. Ravasi, B. Lenhard, C. Wells, R. Kodzius, K. Shimokawa, V. B. Bajic, S. E. Brenner, S. Batalov, A. R. Forrest, M. Zavolan, M. J. Davis, L. G. Wilming, V. Aidinis, J. E. Allen, A. Ambesi-Impiombato, R. Apweiler, R. N. Aturaliya, T. L. Bailey, M. Bansal, L. Baxter, K. W. Beisel, T. Bersano, H. Bono, A. M. Chalk, K. P. Chiu, V. Choudhary, A. Christoffels, D. R. Clutterbuck, M. L. Crowe, E. Dalla, B. P. Dalrymple, B. de Bono, G. Della Gatta, D. di Bernardo, T. Down, P. Engstrom, M. Fagiolini, G. Faulkner, C. F. Fletcher, T. Fukushima, M. Furuno, S. Futaki, M. Gariboldi, P. Georgii-Hemming, T. R. Gingeras, T. Gojobori, R. E. Green, S. Gustincich, M. Harbers, Y. Hayashi, T. K. Hensch, N. Hirokawa, D. Hill, L. Huminiecki, M. Iacono, K. Ikeo, A. Iwama, T. Ishikawa, M. Jakt, A. Kanapin, M. Katoh, Y. Kawasawa, J. Kelso, H. Kitamura, H. Kitano, G. Kollias, S. P. Krishnan, A. Kruger, S. K. Kummerfeld, I. V. Kurochkin, L. F. Lareau, D. Lazarevic, L. Lipovich, J. Liu, S. Liuni, S. McWilliam, M. Madan Babu, M. Madera, L. Marchionni, H. Matsuda, S. Matsuzawa, H. Miki, F. Mignone, S. Miyake, K. Morris, S. Mottagui-Tabar, N. Mulder, N. Nakano, H. Nakauchi, P. Ng, R. Nilsson, S. Nishiguchi, S. Nishikawa, F. Nori, O. Ohara, Y. Okazaki, V. Orlando, K. C. Pang, W. J. Pavan, G. Pavesi, G. Pesole, N. Petrovsky, S. Piazza, J. Reed, J. F. Reid, B. Z. Ring, M. Ringwald, B. Rost, Y. Ruan, S. L. Salzberg, A. Sandelin, C. Schneider, C. Schönbach, K. Sekiguchi, C. A. Semple, S. Seno, L. Sessa, Y. Sheng, Y. Shibata, H. Shimada, K. Shimada, D. Silva, B. Sinclair, S. Sperling, E. Stupka, K. Sugiura, R. Sultana, Y. Takenaka, K. Taki, K. Tammoja, S. L. Tan, S. Tang, M. S. Taylor, J. Tegner, S. A. Teichmann, H. R. Ueda, E. van Nimwegen, R. Verardo, C. L. Wei, K. Yagi, H. Yamanishi, E. Zabarovsky, S. Zhu, A. Zimmer, W. Hide, C. Bult, S. M. Grimmond, R. D. Teasdale, E. T. Liu, V. Brusic, J. Quackenbush, C. Wahlestedt, J. S. Mattick, D. A. Hume, C. Kai, D. Sasaki, Y. Tomaru, S. Fukuda, M. Kanamori-Katayama, M. Suzuki, J. Aoki, T. Arakawa, J. Iida, K. Imamura, M. Itoh, T. Kato, H. Kawaji, N. Kawagashira, T. Kawashima, M. Kojima, S. Kondo, H. Konno, K. Nakano, N. Ninomiya, T. Nishio, M. Okada, C. Plessy, K. Shibata, T. Shiraki, S. Suzuki, M. Tagami, K. Waki, A. Watahiki, Y. Okamura-Oho, H. Suzuki, J. Kawai, Y. Hayashizaki; FANTOM Consortium; RIKEN

Genome Exploration Research Group; Genome Science Group (Genome Network Project Core Group), The transcriptional landscape of the mammalian genome. *Science* **309**, 1559–1563 (2005). Medline doi:10.1126/science.1112014

11. M. Skipper, A. Eccleston, N. Gray, T. Heemels, N. Le Bot, B. Marte, U. Weiss, Presenting the epigenome roadmap. *Nature* **518**, 313 (2015). Medline doi:10.1038/518313a

12. F. Yang, X. S. Huo, S. X. Yuan, L. Zhang, W. P. Zhou, F. Wang, S. H. Sun, Repression of the long noncoding RNA-LET by histone deacetylase 3 contributes to hypoxia-mediated metastasis. *Mol. Cell* **49**, 1083–1096 (2013). Medline doi:10.1016/j.molcel.2013.01.010

13. M. N. Cabili, M. C. Dunagin, P. D. McClanahan, A. Biaesch, O. Padovan-Merhar, A. Regev, J. L. Rinn, A. Raj, Localization and abundance analysis of human lncRNAs at single-cell and single-molecule resolution. *Genome Biol.* **16**, 20 (2015). Medline doi:10.1186/s13059-015-0586-4

14. F. Wang, J. Flanagan, N. Su, L. C. Wang, S. Bui, A. Nielson, X. Wu, H. T. Vo, X. J. Ma, Y. Luo, RNAscope: A novel in situ RNA analysis platform for formalin-fixed, paraffin-embedded tissues. *J. Mol. Diagn.* **14**, 22–29 (2012). Medline doi:10.1016/j.jmoldx.2011.08.002

15. A. A. Salamov, T. Nishikawa, M. B. Swindells, Assessing protein coding region integrity in cDNA sequencing projects. *Bioinformatics* **14**, 384–390 (1998). Medline doi:10.1093/bioinformatics/14.5.384

16. M. Punta, P. C. Coggill, R. Y. Eberhardt, J. Mistry, J. Tate, C. Boursnell, N. Pang, K. Forslund, G. Ceric, J. Clements, A. Heger, L. Holm, E. L. Sonnhammer, S. R. Eddy, A. Bateman, R. D. Finn, The Pfam protein families database. *Nucleic Acids Res.* **40**, D290–D301 (2012). Medline doi:10.1093/nar/gkr1065

17. J. Ernst, Z. Bar-Joseph, STEM: A tool for the analysis of short time series gene expression data. *BMC Bioinformatics* **7**, 191 (2006). Medline doi:10.1186/1471-2105-7-191

18. V. Abadie, V. Discepolo, B. Jabri, Intraepithelial lymphocytes in celiac disease immunopathology. *Semin. Immunopathol.* **34**, 551–566 (2012). Medline doi:10.1007/s00281-012-0316-x

19. N. Periolo, L. Guillén, M. L. Arruvito, N. S. Alegre, S. I. Niveloni, J. H. Hwang, J. C. Bai, A. C. Cherñavsky, IL-15 controls T cell functions through its influence on CD30 and OX40 antigens in celiac disease. *Cytokine* **67**, 44–51 (2014). Medline doi:10.1016/j.cyto.2014.01.004

20. S. Geisler, L. Lojek, A. M. Khalil, K. E. Baker, J. Coller, Decapping of long noncoding RNAs regulates inducible genes. *Mol. Cell* **45**, 279–291 (2012). Medline doi:10.1016/j.molcel.2011.11.025

21. Y. Li, M. Song, M. Kiledjian, Differential utilization of decapping enzymes in mammalian mRNA decay pathways. *RNA* **17**, 419–428 (2011). Medline doi:10.1261/rna.2439811

22. Y. Li, M. G. Song, M. Kiledjian, Transcript-specific decapping and regulated stability by the human Dcp2 decapping protein. *Mol. Cell. Biol.* **28**, 939–948 (2008). Medline doi:10.1128/MCB.01727-07

23. S. Carpenter, D. Aiello, M. K. Atianand, E. P. Ricci, P. Gandhi, L. L. Hall, M. Byron, B. Monks, M. Henry-Bezy, J. B. Lawrence, L. A. O'Neill, M. J. Moore, D. R. Caffrey, K. A. Fitzgerald, A long noncoding RNA mediates both activation and repression of immune response genes. *Science* **341**, 789–792 (2013). Medline doi:10.1126/science.1240925

24. A. M. Khalil, M. Guttman, M. Huarte, M. Garber, A. Raj, D. Rivea Morales, K. Thomas, A. Presser, B. E. Bernstein, A. van Oudenaarden, A. Regev, E. S. Lander, J. L. Rinn, Many human large intergenic noncoding RNAs associate with chromatin-modifying complexes and affect gene expression. *Proc. Natl. Acad. Sci. U.S.A.* **106**, 11667–11672 (2009). Medline doi:10.1073/pnas.0904715106

25. J. Engreitz, E. S. Lander, M. Guttman, RNA antisense purification (RAP) for mapping RNA interactions with chromatin. *Methods Mol. Biol.* **1262**, 183–197 (2015). Medline doi:10.1007/978-1-4939-2253-6_11

26. M. Huarte, M. Guttman, D. Feldser, M. Garber, M. J. Koziol, D. Kenzelmann-Broz, A. M. Khalil, O. Zuk, I. Amit, M. Rabani, L. D. Attardi, A. Regev, E. S. Lander, T. Jacks, J. L. Rinn, A large intergenic noncoding RNA induced by p53 mediates global gene repression in the p53 response. *Cell* **142**, 409–419 (2010). Medline doi:10.1016/j.cell.2010.06.040

27. N. Sadri, R. J. Schneider, Auf1/*Hnrnpd*-deficient mice develop pruritic inflammatory skin disease. *J. Invest. Dermatol.* **129**, 657–670 (2009). Medline doi:10.1038/jid.2008.298

28. C. Lee, A. Gyorgy, D. Maric, N. Sadri, R. J. Schneider, J. L. Barker, M. Lawson, D. V. Agoston, Members of the NuRD chromatin remodeling complex interact with AUF1 in developing cortical neurons. *Cereb. Cortex* **18**, 2909–2919 (2008). Medline doi:10.1093/cercor/bhn051

29. S. Mili, H. J. Shu, Y. Zhao, S. Piñol-Roma, Distinct RNP complexes of shuttling hnRNP proteins with pre-mRNA and mRNA: Candidate intermediates in formation and export of mRNA. *Mol. Cell. Biol.* **21**, 7307–7319 (2001). Medline doi:10.1128/MCB.21.21.7307-7319.2001

30. C. A. McHugh, C. K. Chen, A. Chow, C. F. Surka, C. Tran, P. McDonel, A. Pandya-Jones, M. Blanco, C. Burghard, A. Moradian, M. J. Sweredoski, A. A. Shishkin, J. Su, E. S. Lander, S. Hess, K. Plath, M. Guttman, The *Xist* lncRNA interacts directly with SHARP to silence transcription through HDAC3. *Nature* **521**, 232–236 (2015). Medline doi:10.1038/nature14443

31. G. W. Cox, B. J. Mathieson, L. Gandino, E. Blasi, D. Radzioch, L. Varesio, Heterogeneity of hematopoietic cells immortalized by v-myc/v-raf recombinant retrovirus infection of bone marrow or fetal liver. *J. Natl. Cancer Inst.* **81**, 1492–1496 (1989). Medline doi:10.1093/jnci/81.19.1492

32. G. A. Follows, M. E. Janes, L. Vallier, A. R. Green, B. Gottgens, Real-time PCR mapping of DNaseI-hypersensitive sites using a novel ligation-mediated amplification technique. *Nucleic Acids Res.* **35**, e56 (2007). Medline doi:10.1093/nar/gkm108